Synthesis of Copper-Core/Carbon-Sheath Nanocables by a Surfactant-Assisted Hydrothermal Reduction/Carbonization Process

Bin Deng, An-Wu Xu,* Guang-Yi Chen, Rui-Qi Song, and Liuping Chen

School of Chemistry and Chemical Engineering, Sun Yat-Sen University, Guangzhou 510275, China

Received: January 16, 2006; In Final Form: April 18, 2006

A simple hydrothermal method has been developed for the one-step synthesis of copper-core/carbon-sheath nanocables in solution. The obtained nanostructures were characterized by X-ray diffraction (XRD), transmission electron microscopy (TEM), and high-resolution TEM (HRTEM), Raman, and UV−vis spectrum analysis. These copper@carbon nanocables formed through the hydrothermal reduction/carbonization in the presence of surfactant cetyltrimethylammonium bromide (CTAB) acting as the structure-directing agent by hydrothermal treatment. HRTEM and selected-area electron diffraction (SAED) indicate that the resulted Cu nanowires had the preferred [110] growth direction. The influence of the reaction temperature, reaction time, and pH on the final products was investigated in detail. The possible formation mechanism for copper-core/carbon-sheath nanocables was also proposed. Amorphous carbon nanotubes can be obtained by etching the copper core in the nanocables.

Introduction

Many one-dimensional (1D) nanostructures such as nanowires, nanotubes, and nanocables have been investigated during the past decades, owing to their unique applications in mesoscopic physics and fabrication of nanoscale devices.[1,2] For many purposes, growth of core−shell 1D heterostructures is of critical significance because their functions may be further improved. Some core−shell 1D nanostructures (nanocables) have already been reported.[2]

Metal nanowires have received much attention due to their potential use as interconnects in future nanoelectronics and application possibilities for catalysts, electron emitters, magnetic devices, and so on. The metal copper having a high electrical conductivity has been used in a wide variety of commercial applications and its properties could be enhanced by processing it into various nanostructures with well-controlled dimension. For future bottom-up nanotechnology, the fabrication of 1D copper nanostructures, as a first step toward a nanooptoelectronic device, has attracted considerable attention in recent years, and a number of synthetic routes have been developed, which include electrochemical depositions,[3] vapor−solid reaction growth and vapor depositions,[4] reverse micelle systems,[5] templating processes,[6] etc.[7] Although significant research progress has been made to synthesize copper nanomaterials, to the best of our knowledge, developing a facile approach to large-scale production of copper/carbon nanocables has still been limited to date.

As encouraged by the novel properties of carbon nanomaterials such as carbon fullerenes[8] and carbon nanotubes,[9] substantial effort has been devoted to the search for new synthetic strategies for fabricating carbon nanoarchitectures, nanocomposites, and related materials due to their potential applications in many areas.[10] In addition to direct synthesis, carbon nanocavities can be posteriorly filled with metals and other materials to form nanocomposites with improved functions, which includes filling fullerene-related materials in electric arcs[11] or the combination of an efficient nanotube production method[12] and capillary forces.[13] Carbon nanomaterials were mostly synthesized in low yield by electric-arc discharge, catalytic chemical vapor deposition, and laser vaporization, which usually occurs under high vacuum.[14] More recently, several studies have been reported on the synthesis of carbon nanotubes and amorphous carbon materials by the solution-based method.[15] However, most of the chemical reactions are complicated and uncontrollable.

Herein, we introduce an efficient method for the controlled synthesis of copper/carbon nanocables by a one-pot surfactant-assisted hydrothermal reduction/carbonization process. Although the obtained carbon nanostructures are not as ordered as carbon nanotubes, this is the first report on the large-scale synthesis of copper/carbon nanocables with a high content of carbon under facile aqueous conditions. The main difficulty for the use of pure metals arises from their instability toward oxidation in air and dissolution in acid, which becomes much easier as the size becomes smaller. Moreover, metal nanoparticles agglomerated easily because of their high surface energies. On the other hand, after carbon materials were coated on metal nanoparticles, these nanostructures can be further rationally functionalized by chemical strategies similar to carbon nanotubes functionalization.[16] In our approach, CTAB acted as the structure-directing agent, and metal salts such as $CuSO_4$ acted as the catalyst and source of the metal to be encapsulated. The aqueous hexamethylenetetramine (HMT) solution was mixed with a suitable amount of metal salts and CTAB, and was then hydrothermally treated at 140−160 °C, leading to the formation of novel copper/carbon nanocables. The effect of the reaction temperature, reaction time, and pH on the final products was systematically examined. The structure and compositions of the as-grown coaxial nanocables were investigated, and a growth mechanism was proposed as well. Amorphous carbon nanotubes were further prepared by etching the copper core in the copper/carbon nanocables.

* Address correspondence to this author. Phone: 86-20-84115827. Fax: 86-20-84111088. E-mail: an-wu.Xu@mpikg.mpg.de.

10.1021/jp0603029 CCC: $33.50
Published on Web 05/25/2006

Experimental Section

Preparation. All of the chemical regents used in the experiments were analytical grade. In a typical synthesis, 0.005 mol of $CuSO_4$, 0.005 mol of hexamethylenetetramine (HMT), and 0.4 g of cetyltrimethylammonium bromide (CTAB) were first dissolved in 12 mL of water under stirring, then 5 mL of aqueous ammonia (25 wt %) was added to the above solution. The resulting homogeneous solution having pH 11 was poured into a Teflon-lined stainless steel autoclave (capacity, 20 mL), then sealed and maintained in an oven at 130−200 °C for 2−48 h. After the reaction was completed, the resulting solid product was filtered, washed with distilled water and absolute alcohol to remove ions possibly remaining in the final products, and finally dried at 80 °C in air.

Characterization. The X-ray powder diffraction (XRD) patterns of the samples were performed on a Rigaku/Max-3A X-ray diffractometer with Cu Kα radiation (λ = 1.54178 Å), the operation voltage and current maintained at 40 kV and 40 mA, respectively. Field emission scanning electron microscopic (FE-SEM) images were obtained with a JEOL JSM-6330F operated at a beam energy of 15.0 kV. Transmission electron microscopic (TEM) images, high-resolution transmission electron microscopic (HRTEM) images, and the selected area electron diffraction (SAED) patterns were performed on a JEOL-2010 microscope with an accelerating voltage of 200 kV. Energy-dispersive X-ray spectroscopy (EDS) is attached to the JEOL 2010. Sample grids were prepared by sonicating powdered samples in ethanol for 20 min and evaporating one drop of the suspension onto a carbon-coated, holey film supported on a copper grid for TEM measurements. X-ray photoelectron spectroscopy (XPS) measurements were carried out on a VG Scientific ESCALAB Mark II spectrometer equipped with two ultrahigh-vaccum (UHV) chambers. All binding energies were referenced to the C1s peak at 284.6 eV of the surface adventitious carbon. The Raman spectrum was recorded at room temperature on a LABRAM-HR Confocal Laser MicroRaman spectrometer. Elemental analysis of carbon and hydrogen was performed at the Analysis Center of Sun Yat-Sen University. A Shimadzu spectrophotometer (Model 2501 PC) equipped with an integrating sphere was used to record the UV−vis diffuse reflectance spectra of the samples.

Results and Discussion

The phase and purity of the as-obtained products was determined from the XRD measurements. The XRD pattern of the obtained Cu@C core−shell nanocables prepared by hydrothermal treatment at 150 °C for 48 h is shown in Figure 1. All the peaks of the XRD pattern for the sample in Figure 1 can be readily indexed to a cubic phase of Cu crystals; the reflection peaks at 2θ = 43.4, 50.6, and 74.2 are indexed as [111], [200], and [220] planes of copper, respectively, in good agreement with the reported data (JCPDS No. 4-836, a = 0.3615 nm). The calculated lattice parameter (a) of a unit cell is estimated to be 0.362 nm. The rather sharp diffraction peaks suggest a high crystallinity of copper crystals.

The morphology and dimension of the as-prepared products were examined by FESEM. The SEM image in Figure 2a shows that the product is mainly composed of copper/carbon nanocables with lengths as long as 40 μm and diameters of 80−400 nm prepared at 150 °C for 48 h. It has to be mentioned that some of the produced nanocables tend to branch or fuse with each other and some nanocables bent at a nearly 90° angle (pointed to by arrows in Figure 2a). An incompletely filled tube and a cable with a bare core head are shown in the inset in

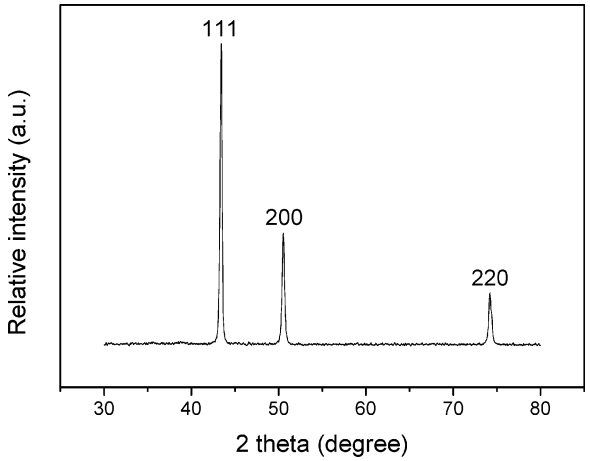

Figure 1. The XRD pattern of the obtained Cu@C nanocables under hydrothermal treatment at 150 °C for 48 h.

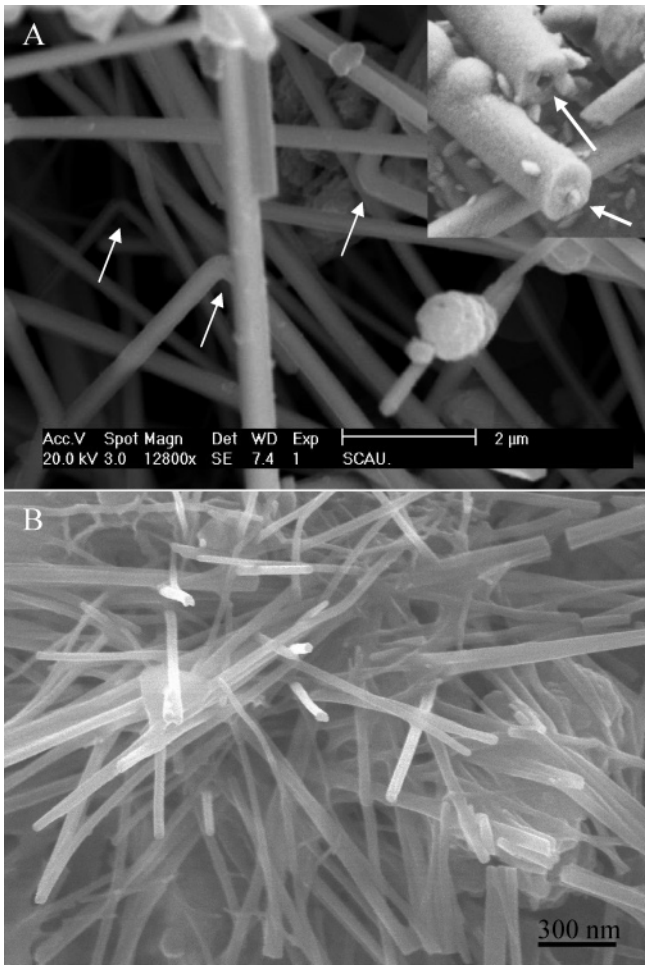

Figure 2. SEM images of the as-made Cu@C nanocables grown by hydrothermal treatment at 150 °C for 48 h (a) and 140 °C for 30 h (b).

Figure 2a (pointed to by arrows). A small portion of carbon spheres can also be observed in the product. The nanocables with a diameter of 30−90 nm can be obtained by hydrothermal treatment at 140 °C for 30 h, as seen in Figure 2b.

The microstructures of the obtained samples were further examined with transmission electron microscopy (TEM), high-resolution transmission electron microscopy (HRTEM), and selected area electron diffraction (SAED). Typical TEM images of Cu@C nanocables are shown in Figure 3a−c. Light and dark contrast is clearly observed along the radial direction. The

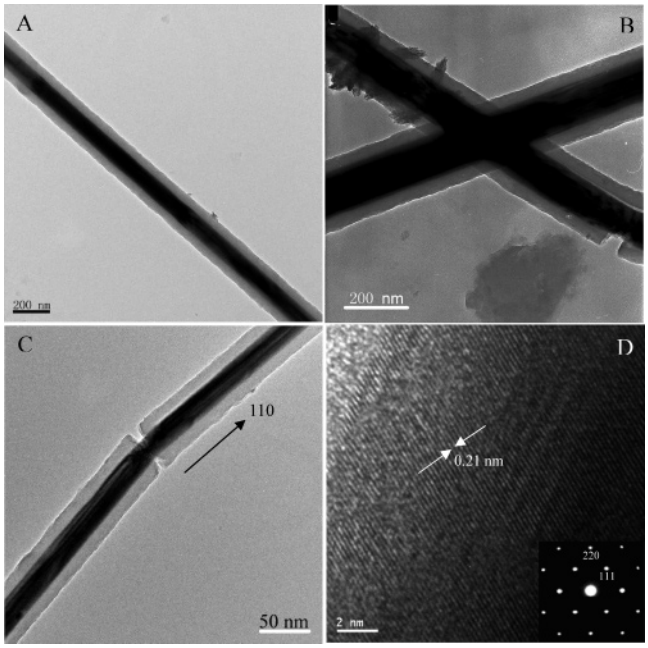

Figure 3. TEM images (a−c) and HRTEM image (d) of the products obtained under hydrothermal treatment at 150 °C for 48 h and 140 °C for 30 h (c). The inset in part d is the SAED pattern taken from the [−110] zone axis.

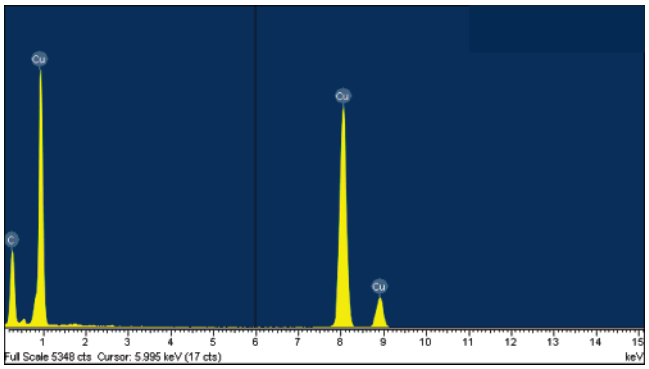

Figure 4. EDS spectrum of the as-prepared copper@carbon nanocables.

different contrast suggests a different phase composition, indicating the core−sheath cable structure. The dark contrast suggests Cu crystals with larger mass thickness in the core region. Outside of the core region, the light contrast suggests that the sheath layer is carbon. Figure 3d shows a typical HRTEM image of an individual Cu@C nanocable, giving resolved lattice fringes of (111) planes (d_{111} = 0.21 nm); the growth of the nanocable is along the [110] direction. The SAED pattern (the inset in Figure 3d) taken from this nanocable can be indexed as a cubic copper single-crystal recorded from the [−110] zone axis. Energy-dispersive X-ray spectroscopy (EDS) analysis measured from nanocables shows that the nanocables are composed of copper and carbon elements (Figure 4). The Raman spectrum analysis of the obtained sample (Figure 5) shows two broad peaks appearing at 1385 and 1585 cm^{-1}, which is very similar to the spectrum of the sp^2 carbon-bonded amorphous carbon.[17]

The surface information of the freshly obtained sample as shown in Figure 6 can be properly provided by XPS analysis. The binding energies obtained in XPS analysis were corrected with the reference to C1s (284.6 eV). The core-level spectrum of Cu 2p (Figure 6) illustrates that the observed value of the binding energy for Cu $2p_{3/2}$ (932.2 eV) is consistent with the

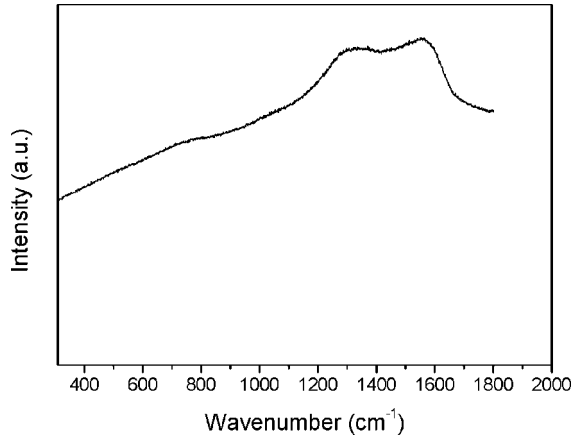

Figure 5. Raman spectrum of the as-prepared Cu@carbon nanocables.

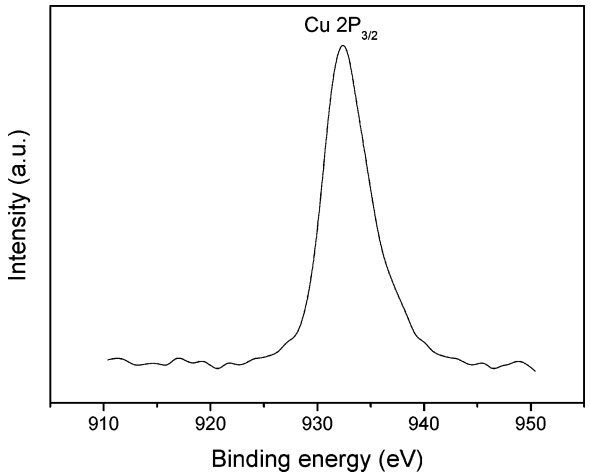

Figure 6. The XPS spectrum of the obtained Cu@carbon nanocables.

reported data for Cu^0.[18] All the above results demonstrate that the obtained samples have indeed 1D core−shell nanostructures with the core of copper and the shell of amorphous carbon.

The effects of reaction temperature, pH, and hydrothermal reaction time on the final products were systematically studied. Controlled experiments showed that Cu@C cables were obtained under proper experimental conditions. If reaction conditions such as reaction temperature and/or pH were changed, the Cu_2O phase was observed, and the final product was a mixture of Cu, Cu_2O, and amorphous C. It has been found that the pH of the initial mixture of the solution influenced the final products significantly. When pH was lower than 9 while other conditions were kept identical, a mixture of Cu and Cu_2O was obtained, as shown in Figure 7a. The optimal pH for the formation of Cu@C cables was found to in the range of 10−12. On the other hand, when the reaction temperature was increased to 200 °C, Cu_2O was obtained, and the final product is a mixture of Cu and Cu_2O, as shown in Figure 7b. The SEM image shows that Cu_2O particles have octahedral morphology (Figure 8), usually observed for Cu_2O crystals.[19] While reaction temperature was lower than 130 °C, no Cu@C cables were obtained.

The effect of the reaction time on the final products was also investigated. When the reaction time was 2 h while other conditions were kept constant, the XRD pattern shows that no Cu phase was obtained (Figure 9a). When the reaction time was increased to 7 and 12 h, the Cu phase was observed, as is clearly seen in Figure 9, parts b and c, respectively. However, Cu crystals show irregular particle morphology and poor crystallinity. Figure 10 shows the SEM image of the sample prepared at a reaction time of 12 h. Irregular particles are Cu

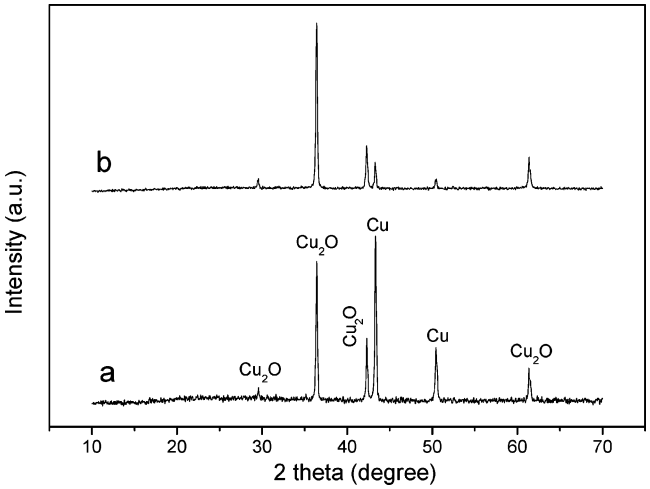

Figure 7. The XRD patterns of the obtained products under hydrothermal treatment: (a) initial pH 9 and (b) 200 °C for 24 h.

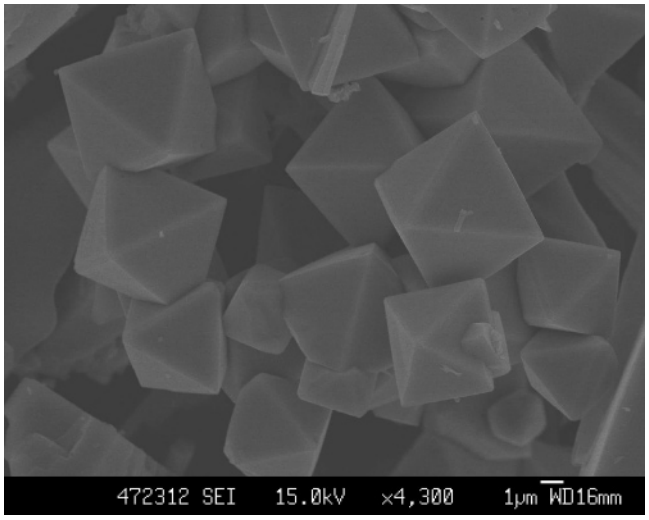

Figure 8. SEM image of the product obtained by hydrothermal treatment at 200 °C for 24 h.

crystals, and nanotubes are amorphous C, as demonstrated by TEM measurements. Cu@C cable structures only appeared after reaction time exceeded 12 h.

The proposed formation mechanism of copper-core/carbon-sheath nanocables can be best explained based on the following reactions. It is known that HMT can be decomposed into formaldehyde and ammonia under hydrothermal treatment.[20] Self-oxidation−reduction reactions in the autoclave possibly take place under hydrothermal conditions at elevated temperatures. The derived formaldehyde (HCHO) can reduce Cu^{2+} into Cu element under hydrothermal conditions,[21] as indicated in the following reaction equations

$$C_6H_{12}N_4\,(\mathrm{HMT}) + 6H_2O \rightarrow 6HCHO + 4NH_3 \qquad (1)$$

$$2Cu^{2+} + HCHO + 2H_2O + 6NH_3 \rightarrow 2Cu + CO_3^{2-} + 6NH_4^{+} \qquad (2)$$

To demonstrate reduction of Cu^{2+} into Cu by HCHO under hydrothermal conditions, HCHO was used in the reaction system instead of HMT, as shown in Figure 11, and the Cu phase was obtained when using HCHO instead of HMT.

When the reaction was performed in the absence of CTAB, almost irregular Cu particles were observed, as is clearly shown

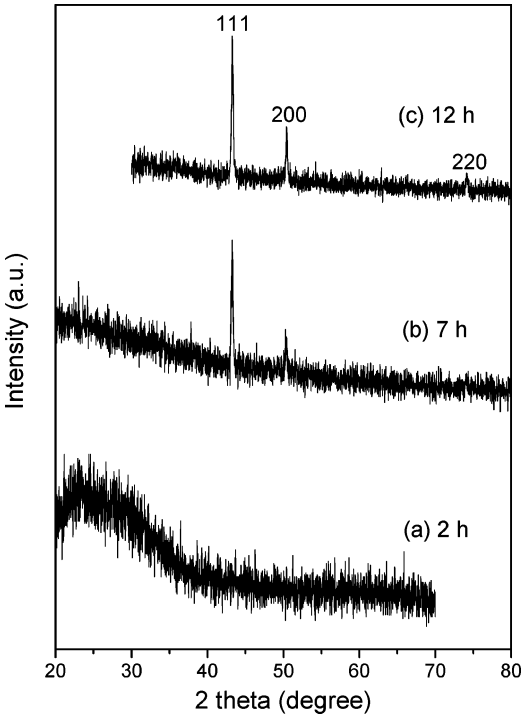

Figure 9. The XRD patterns of the products prepared at different reaction times under hydrothermal treatment at 150 °C: (a) 2, (b) 7, and (c) 12 h.

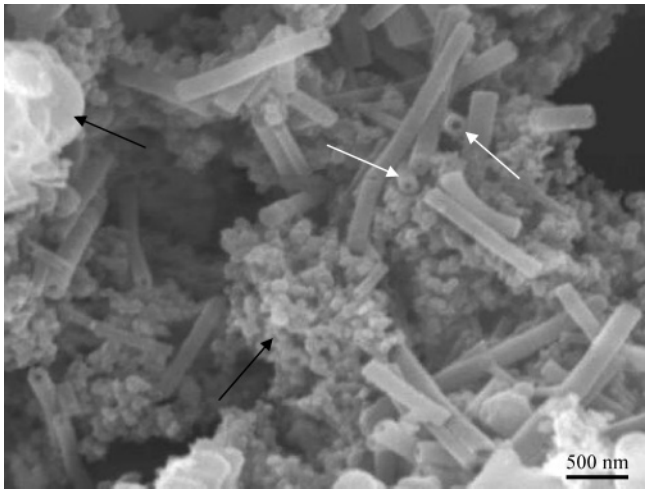

Figure 10. SEM image of the product prepared by hydrothermal treatment at 150 °C for 12 h. White arrows point to amorphous C nanotubes, while black arrows point to irregular Cu particles.

in the SEM image (Figure 12), indicating that CTAB plays an important role in the formation of the 1D nanostructure. From Figure 12 it can be seen that a few rodlike particles exist in the final products. TEM measurements demonstrate that these rods have Cu@C core−shell structure, indicating that amorphous C most likely comes from HMT decomposition under hydrothermal conditions, and derived amorphous carbon coated on Cu nanowires to form the final Cu@carbon nanocables. Here, CTAB has a template effect on the formation of 1D nanocables acting as the directing agent for 1D nanostructures.

The previous studies demonstrated that the presence of CTAB was found to be helpful for the formation of different types of 1D nanostructures, such as Au,[22] ZnO,[23] and Cu_2O and CuO.[24] As the structure-directing agent, it could be believed that the presence of surfactant CTAB prevents the aggregation of Cu nanoparticles in the initial stage of nanowire growth and

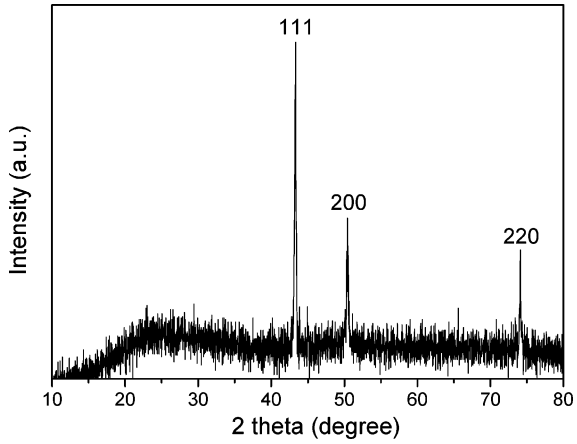

Figure 11. The XRD pattern of the obtained product under hydrothermal treatment with HCHO instead of HMT while other conditions were kept identical.

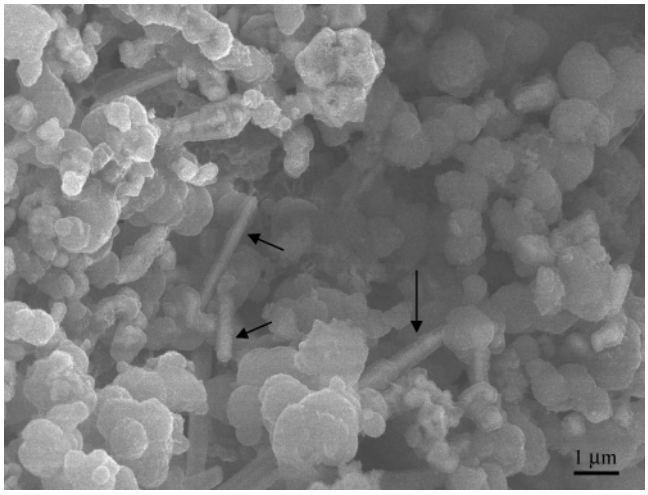

Figure 12. SEM image of the product obtained in the absence of CTAB by hydrothermal treatment. Black arrows point to Cu@C cables.

kinetically controls the growth rates of different crystallographic faces of face-centered cubic Cu through selectively adsorbing on these faces. In this case, the roles of CTAB on the formation of Cu nanowires were similar to these of poly(vinylpyrrolidone) (PVP) on the formation of Ag and Pb nanowires.[25] In the absence of CTAB, the reaction only produced many irregular particles of several micrometers, which often appeared as particle aggregates. This indicates that the initially formed copper nanoparticles had a strong tendency to aggregate as larger ones when no protective agents were added. When CTAB was introduced in appropriate amounts, the initially formed nanoparticles were relatively small in dimension, and well dispersed in the solution. The selective adsorption of CTAB on specific crystal faces promotes Cu crystals to grow along the [110] direction forming the final nanostructures.

The absorption spectrum of the as-prepared copper@carbon nanocables dispersed in ethanol is shown in Figure 13. A broad absorption band with a maximum at 566 nm is observed, which is in good agreement with the reported values for copper nanoparticles,[26] and this is attributable to the plasma excitation in copper nanowires. The result also indicates that the thin carbon shells on the surfaces of Cu nanowires had little effect on the absorption edge.

No graphitic carbon layers were observed by high-resolution TEM measurements for the as-synthesized samples. However, further thermal treatment of the as-obtained sample at 550 °C

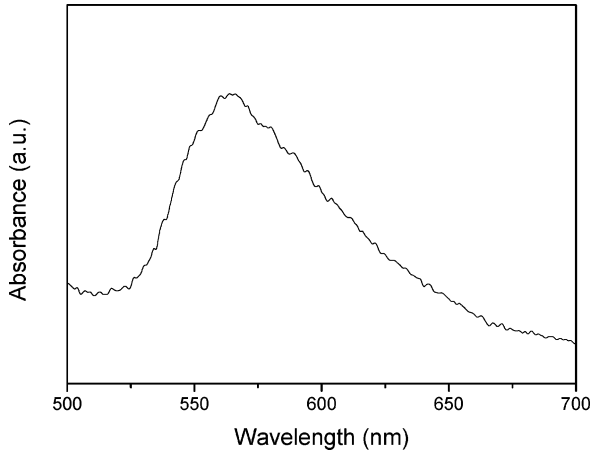

Figure 13. UV−vis absorption spectrum of the as-obtained Cu@carbon nanocables.

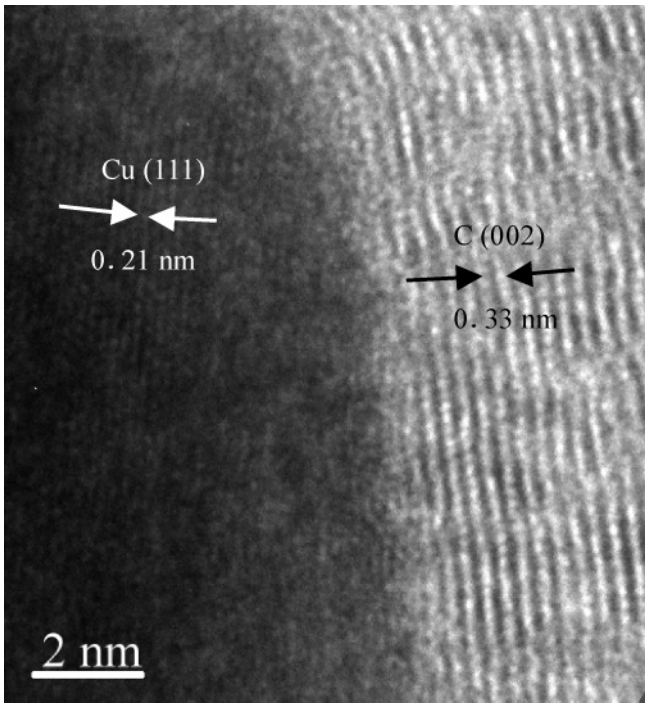

Figure 14. HRTEM image of the copper/carbon interface close to the tip of a single nanocable. The product was first hydrothermally treated at 150 °C for 48 h, then sintered at 600 °C for 10 h under vacuum.

for 10 h under vacuum produced the graphitic structure. The HRTEM image (Figure 14) taken from the core/sheath interface clearly shows the well-resolved copper (111) lattice space of 0.21 nm, and a kind of graphitic carbon with a 0.33 nm layer-to-layer distance,[27] with the graphene layers oriented nearly parallel to the interface.

Carbon nanotubes can be obtained from copper/carbon nanocables through etching the core with concentrated HNO_3 solution. Figure 15a clearly shows the tubular structure of carbon. The HRTEM image is shown in Figure 15b, demonstrating the amorphous nature of disordered carbon nanotubes.

Conclusions

In summary, we have introduced a new one-step approach to prepare copper-core/carbon-sheath nanocables by the hydrothermal method. In practice, the formation of copper-core/carbon-sheath nanocables was performed through the hydrothermal reduction/carbonization with CTAB acting as a structure-

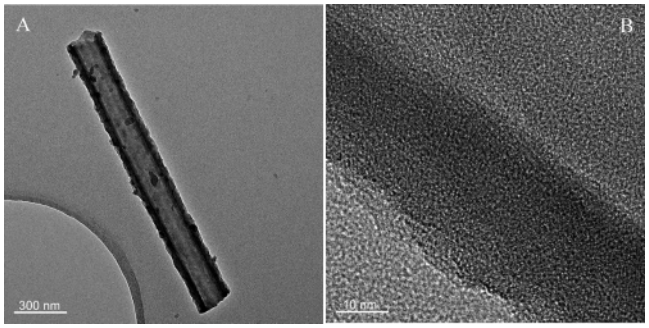

Figure 15. TEM (a) and HRTEM (b) images of the amorphous carbon nanotubes prepared by etching the copper core in Cu@carbon nanocables with concentrated HNO_3 solution.

directing agent. The formation of Cu@carbon nanocables was clearly demonstrated by XRD pattern, TEM measurements, and Raman spectrum analysis. This simple and facile process is favorable for the future bulk synthesis and functionalization of various carbon-related nanomaterials of technical importance. Coaxial nanocables consist of highly conducting metallic cores and relatively insulating sheathes could be used as components and interconnects in nanoelectronic devices. Further extension of this approach and investigation of the properties of this new kind of 1D nanocables are ongoing.

Acknowledgment. Support from the National Natural Science Foundation of China (20371053) and the Guangdong Province NSF (031574) is gratefully acknowledged.

References and Notes

(1) (a) Xia, Y.; Yang, P.; Sun, Y.; Wu, Y.; Mayers, B.; Gates, B.; Yin, Y.; Kim, F.; Yan, H. *Adv. Mater.* **2003**, *15*, 353. (b) Tenne, R. *Angew. Chem., Int. Ed.* **2003**, *42*, 5124. (c) Xu, A. W.; Fang, Y. P.; You, L. P.; Liu, H. Q. *J. Am. Chem. Soc.* **2003**, *125*, 1494. (d) Goldberger, J.; He, R.; Zhang, Y. F.; Lee, S.; Yan, H.; Choi, H. J.; Yang, P. *Nature* **2003**, *422*, 599.

(2) (a) Lauhon, L. J.; Gudiksen, M. S.; Wang, D. L.; Lieber, C. M. *Nature* **2002**, *420*, 57. (b) Yu, S. H.; Cui, X. J.; Li, L. L.; Li, K.; Yu, B.; Antonietti, M.; Cölfen, H. *Adv. Mater.* **2004**, *16*, 1636. (c) Jang, J.; Lim, B.; Lee J.; Hyeon, T. *Chem. Commun.* **2001**, 83. (d) Fang, Y. P.; Xu, A. W.; Dong, W. F. *Small* **2005**, *1*, 967. (e) Li, Q.; Wang, C. R. *J. Am. Chem. Soc.* **2003**, *125*, 9892. (f) Obare, S. O.; Jana N. R.; Murphy, C. J. *Nano Lett.* **2001**, *1*, 601.

(3) (a) Molares, M. E. T.; Buschamann, V.; Dobrev, D.; Scholz, R.; Schuchert, I. U.; Vetter, J. *Adv. Mater.* **2001**, *13*, 62. (b) Choi, H.; Park, S. H. *J. Am. Chem. Soc*. **2004**, *126*, 6248.

(4) Liu, Z.; Bando, Y. *Adv. Mater.* **2003**, *15*, 303.

(5) Pileni, M. P.; Gulik-Krzywicki, T.; Tanori, J.; Filankembo, A.; Dedieu, J. C. *Langmuir* **1998**, *14*, 7359−7363.

(6) (a) Monson, C. F.; Woolley, A. T. *Nano Lett.* **2003**, *3*, 359. (b) Liu, Z.; Yang, Y.; Liang, J.; Hu, Z.; Li, S.; Peng, S.; Qian, Y. *J. Phys. Chem. B* **2003**, *107*, 12658. (c) Yen, M.-Y.; Chiu, C.-W.; Hsia, C.-H.; Chen, F.-R.; Kai, J.-J.; Lee, C.-Y.; Chiu, H.-T. *Adv. Mater.* **2003**, *15*, 235.

(7) (a) Cao, X. B.; Yu, F.; Li, L. Y.; Yao, Z. Y.; Xie, Y. *J. Cryst. Growth* **2003**, *254*, 164. (b) Dhas, N. A.; Raj, C. P.; Gedanken, A. *Chem. Mater.* **1998**, *10*, 1446. (c) Zhang, D. W.; Chen, C. H.; Zhang, J.; Ren, F. *Chem. Mater.* **2005**, *17*, 5242.

(8) Kroto, H. W.; Heath, J. R.; O'Brien, S. C.; Curl, R. F.; Smalley, R. E. *Nature* **1985**, *318*, 162.

(9) Iijima, S. *Nature* **1991**, *354*, 56.

(10) (a) Ding, L. H.; Olesik, S. V. *Nano Lett.* **2004**, *4*, 2271. (b) Burda, C.; Chen, X. B.; Narayanan, R.; El-Sayed, M. A. *Chem. Rev.* **2005**, *105*, 1025. (c) Saito, R.; Dresselhaus, G.; Dresselhaus, M. S. *Physical Properties of Carbon Nanotubes*; Imperial College Press: London, UK, 1998.

(11) (a) Smith, B. W.; Monthioux, M.; Luzzi, D. E. *Nature* **1998**, *396*, 323. (b) Ruoff, R. S.; Lorents, D. C.; Chan, B.; Malhotra, B.; Subramoney, S. *Science* **1993**, *259*, 346.

(12) Ebbesen, T. W.; Ajayan, P. M. *Nature* **1992**, *358*, 220.

(13) Ugarte, D.; Châtelain, A.; de Heer, W. A. *Science* **1996**, *274*, 1897.

(14) (a) Journet, C.; Maser, W. K.; Bernier, P.; Louiseau, A.; Chapelle, M. L.; Lefrant, S.; Lee, R.; Fischer, J. E. *Nature* **1997**, *388*, 756. (b) Jose-Yacaman, M.; Miki-Yoshida, M.; Rendon, L.; Santiesteban, J. G. *Appl. Phys. Lett.* **1993**, *62*, 657. (c) Guo, T.; Nikolaev, P.; Thess, A.; Colbert, D. T.; Smalley, R. E. *Chem. Phys. Lett*. **1995**, *243*, 49.

(15) (a) Motiei, M.; Haclhen, Y. R.; Calderon-Moreno, J.; Gedanken, A. *J. Am. Chem. Soc*. **2001**, *123*, 8624. (b) Lee, D. E.; Mikulec, F. V.; Korgel, B. A. *J. Am. Chem. Soc*. **2004**, *126*, 4951.

(16) Sun Y. P.; Fu, K. F.; Lin, Y.; Huang, W. J. *Acc. Chem. Res.* **2002**, *35*, 1096.

(17) Robertson, J. In *Graphite and Precursors*; Delhaes, P., Ed.; Gordon and Breach Science Publishers: Singapore, 2001; p 256.

(18) Chang, Y.; Lye, M. L.; Zeng, H. C. *Langmuir* **2005**, *21*, 3746.

(19) Kostov, I. Mineralogy, Oliver and Boyd: Edinburgh, London, UK, 1968; p 257.

(20) Govender, K.; Boyle, D. S.; Kenway, P. B.; O'Brien, P. *J. Mater. Chem.* **2004**, *14*, 2575.

(21) (a) Yu, D. B.; Yam, V. W.-W. *J. Am. Chem. Soc.* **2004**, *126*, 13200. (b) Chen, Z. Z.; Shi, E. W.; Zheng, Y. Q.; Li, W. J.; Xiao, B.; Zhuang, J. R. *J. Cryst. Growth* **2003**, *249*, 294.

(22) Johnson, C. J.; Dujardin, E.; Davis, S. A.; Murphy, C. J.; Mann, S. *J. Mater. Chem.* **2002**, *12*, 1765.

(23) Zhang, H.; Yang, D. R.; Ji, Y. J.; Ma, X. Y.; Xu, J.; Que, D. L. *J. Phys. Chem. B* **2004**, *108*, 3956.

(24) Cao, M. H.; Hu, C. W.; Wang, Y. H.; Guo, Y. H.; Guo, C. X.; Wang, E. B. *Chem. Commun.* **2003**, 1884.

(25) (a) Sun, Y. G.; Gates, B.; Mayers, B.; Xia, Y. N. *Nano Lett.* **2002**, *2*, 165. (b) Wang, Y. L.; Herricks, T.; Xia, Y. N. *Nano Lett.* **2003**, *3*, 1163.

(26) Joanna, P.; Cason, M. E.; Thompson, B. J.; Roberts, C. B. *J. Phys. Chem. B* **2001**, *105*, 2297.

(27) Ajayan, P. M. *Chem. Rev.* **1999**, *99*, 1787.